Low Loss, Compact TM-Pass Polarizer Based on Hybrid Plasmonic Grating

Bowen Bai, *Student Member, IEEE*, Lu Liu, Ruixuan Chen, and Zhiping Zhou, *Senior Member, IEEE*

***Abstract*— A low-loss, compact TM-pass polarizer is demonstrated based on hybrid plasmonic grating on silicon-on-insulator platform. Since the large mode distribution mismatch and plasmonic effect significantly influence the transmission and reflection spectrum of the device, the traditional theory of Bragg grating cannot fully explain this phenomenon. Here, we proposed an analysis method which takes effective index and mode overlap together into consideration to design this polarizer. A compact length of 2.5 μm with extinction ratio over 25 dB is realized simultaneously. Moreover, the insertion loss is only 0.088 dB, which is comparable to dielectric-based devices.**

***Index Terms*— Hybird plasmonic grating (HPG), on-chip polarizer, polarization sensitive devices.**

I. Introduction

SILICON-ON-INSULATOR (SOI) platform is prevailing for photonic integrated circuits. The high index contrast enables the possibility of compact footprint; however, it also raises a huge challenge—the performance of the device is highly dependent on the polarization state. To tackle this issue, one solution is using polarization independent devices [1], [2]. Another is introducing polarization diversity scheme [3] where polarization splitters [4] and polarization rotators [5], [6] are essential components. On-chip polarizers, serving as the third approach, are simple and effective devices that can filter unexpected polarizations and retain only one in a system, which play vital roles in a wide range of applications such as communications [3] and bio-sensing [7]. Basically, the principle of a polarizer is to make a structure a good supporter for one polarization while being lossy or cutoff for other polarizations. Traditionally, polarizers are realized based on dielectric schemes [8]–[16]. For example, a shallowly-etched SOI optical waveguide was used to achieve a polarizer [10] with the device length of 1 mm. In order to render TM or TE polarized light pass, [13] proposed a polarizer based on lithium niobate ($LiNbO_3$) waveguide and the length of the device is also 1 mm. Although subwavelength grating is introduced in [16], the length of the structure is as long as 60 μm. Because dielectric structures have relative low birefringence, long device size is needed to accumulate strong polarization effect. Therefore, these devices usually suffer large device length. As the level of integration for photonics system develops rapidly, minimizing the device size is becoming increasingly urgent.

In recent years, due to the unique properties of nanoscale confinement [17] and polarization sensitivity, surface plasmon polaritons (SPPs) has been introduced to realize polarization manipulation devices, such as polarization splitters [18], polarization rotators, and also polarizers [19]–[28]. However, in most cases, plasmonic devices are difficult to fabricate and suffer high insertion loss (IL). For example, metal–insulator–metal (MIM) structures [19], [20], [26] were introduced to realize compact size, but they are difficult to fabricate with planar integrated technology. Polarizers using hybrid plasmonic waveguide (HPW) [21]–[24] usually have large ILs (e.g., 3.2 dB in [21] and 3 dB in [22]), which is not attractive in terms of energy conservation. Although grating structures based on HPW, or hybrid plasmonic grating (HPG) have been reported [25], [27], [28] in order to improve the performance, the ILs are still unneglectable and the sizes are not compact enough. For example, a TE-pass polarizer based on HPG by etching the top SiO_2 layer was proposed in [28]. The device is about 5 μm in length with an IL of 1.36 dB.

In this work, we proposed a low loss, compact HPG based TM-pass polarizer for SOI platform. Not only mode effective index but also mode overlap is taken into consideration in order to realize low IL (0.088 dB) and compact size (2.5 μm) simultaneously. This analysis method is particularly suitable for designing HPG based devices because the large mode distribution mismatch and SPP stimulation show significant impact on transmission and reflection spectrum. Moreover, an extinction ratio (ER) over 25 dB at 1.55 μm wavelength was achieved by carefully choosing the grating period and metal length.

II. Structure and Principle

The proposed device is built on a SOI platform as shown in Fig. 1, it consists of two identical input and output single mode Si waveguides with $h_{si} = 340$ nm in height and a HPG as the polarizer section in between. The HPG structure is the key part of the device which composes of a Si core with a width of W, and a metal grating with 5 periods. The strips in this grating are of width $W_m = 1$ μm, height h_m and length d. Here, Ag is chosen as the metal material as an example. The gap between the Ag layer and the Si core is g. In principle, certain conditions should be satisfied in order to realize a TM-pass polarizer: a) TM mode could pass through with low loss; b) TE mode is not supported or very lossy. These conditions look straightforward but are very difficult to realize in normal Si waveguides with compact footprint because of the weak birefringence. Fortunately, HPG could support TM mode with low loss while reflecting TE mode. The amount of reflection per unit length, defined as coupling coefficient [29], can be

Manuscript received November 28, 2016; revised January 6, 2017; accepted January 30, 2017. Date of publication February 2, 2017; date of current version March 14, 2017. This work was supported by the National Natural Science Foundation of China under Grant 61377049. *(Corresponding author: Zhiping Zhou.)*

The authors are with the State Key Laboratory of Advanced Optical Communication Systems and Networks, School of Electronics Engineering and Computer Science, Peking University, Beijing 100871, China (e-mail: bowenbai@pku.edu.cn; luliuspm@pku.edu.cn; rxchen@pku.edu.cn; zjzhou@pku.edu.cn).

Color versions of one or more of the figures in this letter are available online at http://ieeexplore.ieee.org.

Digital Object Identifier 10.1109/LPT.2017.2663439

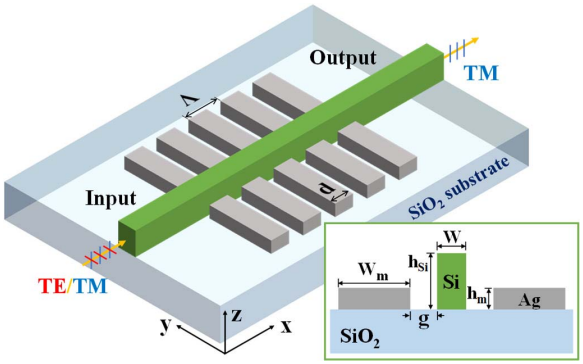

Fig. 1. 3D schematics of proposed TM-pass polarizer. The device is fabricated on SOI platform. Inset: the cross section of the HPG region.

expressed as $\kappa = 2\Delta n_{eff}/(n_{eff}\Lambda)$ in traditional Bragg grating. Here, n_{eff}, Δn_{eff} and Λ are the mode effective index, mode effective indices difference (n_{eff_HPW}-n_{eff_DW}) and grating period, respectively. In order to avoid significant reflection for TM mode, Δn_{eff} should be as small as possible, which is conversely for TE mode. The absolute value of real[Δn_{eff}] for both polarizations are calculated as a function of Si core width W (Fig. 2) using finite element method (FEM). For TE mode, Δn_{eff} increases drastically as g and Wdecreases. TE mode will be reflected by HPG in several periods when choosing small g and W. However, for TM mode, Δn_{eff} is insensitive to g variation. Since Δn_{eff} raises slowly as Wreduces, small W will enlarge the propagation loss for TM mode. Therefore, we choose $g = 50$ nm and $W = 280$ nm as a trade-off.

The height of the metal layer also significantly influences Δn_{eff}. Fig. 3(a) shows the real part of Δn_{eff} for DW and HPW with TM and TE polarization as a function of metal height h_m. Since Δn_{eff} increases with the rise of h_m for both TE and TM mode, if we choose a larger h_m, TE mode can be reflected by HPG in a short length. However, for TM mode, the reflection loss will also raise because of the increased Δn_{eff}. It appears to be a contradiction between low IL and compact footprint from the perspective of Δn_{eff}. Actually, above analysis method is only suitable for TM mode because the mode distributions between two grating steps are similar enough. However, for TE mode, the transmission loss induced by large mode distribution mismatch cannot be ignored. In traditional shallow-etched dielectric based Bragg gratings, mode distribution similarity is so high that the influence of mode overlap is negligible. Δn_{eff}, or longitudinal propagation constant, determines the transmission and reflection spectra. However, mode overlap, from the aspect of transverse propagation constant, shows a significant impact on coupling coefficient for TE mode because of the large mode distribution mismatch and SPPs stimulation in this structure. Thus, not only Δn_{eff} but also mode overlap ratio should be taken into consideration, especially when designing HPG based devices.

Accordingly, mode overlap ratio (Γ) [1] that is theoretically derived from the orthonormal relation of eigenmodes is used to solve this problem. Assuming $\{E_{tu}, H_{tu}\}$ and $\{E_{tv}, H_{tv}\}$ are normalized transverse optical fields of two eigenmodes in DW propagating along + z direction with propagation constant β_u and β_v respectively, they will satisfy the orthonormal relation:

$$\frac{1}{4}\iint\left[\vec{E}_{tu}\times\vec{H}^{*}_{tv}+\vec{E}^{*}_{tv}\times\vec{H}_{tu}\right]_z dxdy=\delta_{u,v} \quad (1)$$

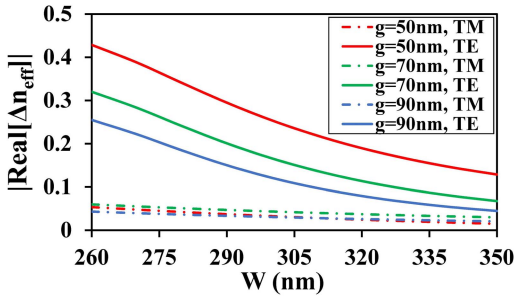

Fig. 2. The absolute value of real part Δn_{eff} for DW and HPW with TM and TE polarization as a function of waveguide width W. Here, $h_m = 170$ nm, $g = 50$ nm, 70 nm and 90 nm, respectively.

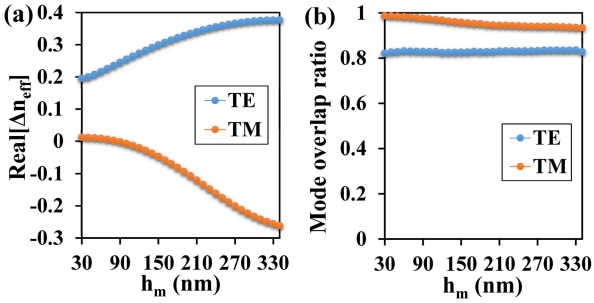

Fig. 3. (a) The real part of mode effective indices difference for DW and HPW with TM and TE polarization as a function of metal height h_m. (b) Mode overlap ratio between the optical field in the HPG region and the fundamental eigenmode in DW as a function of metal height h_m. Here, $W = 280$ nm, and $g = 50$ nm.

where $[\ ]_z$ represents the component of a vector in z-direction, and $\delta_{u,v}$ is Kronecker delta function. All eigenmodes in DW constitute a system of complete orthogonal functions. It means that optical field $\{E_{tm}, H_{tm}\}$ propagating in HPW can be expressed as the superposition of the eigenmodes:

$$\vec{E}_{tm}=\sum_u a_u\vec{E}_{tu}\cdot\exp(-j\beta_u z),\vec{H}_{tm}=\sum_u a_u\vec{H}_{tu}\cdot\exp(-j\beta_u z) \quad (2)$$

The mode expansion coefficient (α_u) can be expressed as follows based on Eq. (1):

$$a_u\cdot\exp(-j\beta_u z)=b_u=\frac{1}{4}\iint\left[\vec{E}_{tm}\times\vec{H}^{*}_{tu}+\vec{E}^{*}_{tu}\times\vec{H}_{tm}\right]_z dxdy \quad (3)$$

$\gamma_u = |\alpha_u|^2 = |b_u|^2$ represents the optical power flow in eigenmode $\{E_{tu}, H_{tu}\}$. By normalizing γ_u with respect to the optical power flow of $\{E_{tm}, H_{tm}\}$, we can get the mode overlap ratio (Γ) between the optical field $\{E_{tm}, H_{tm}\}$ propagating in HPW and the eigenmode field $\{E_{tu}, H_{tu}\}$ in DW from equation (4), shown at the bottom of the next page. The result (Fig. 3(b)) shows that the similarity of optical field distribution gets higher with smaller h_m for TM mode. However, for TE mode, Γ remains almost unchanged as h_m varies. This is because the main component of electric field for TM mode (Fig. 4(c)) is parallel to the metal interface and thus SPP mode cannot be stimulated effectively (Fig. 4(d)). While for hybrid TE mode, SPPs mode are well stimulated so that the optical field are confined in the slot (Fig. 4(b)). The TE mode distribution in DW (Fig. 4(a)) and HPW are quite different due to the plasmonic effect. Although Δn_{eff} will reduce if choosing a small h_m for TE mode, small mode overlap ratio (large mode mismatch) can lead to significant scattering and

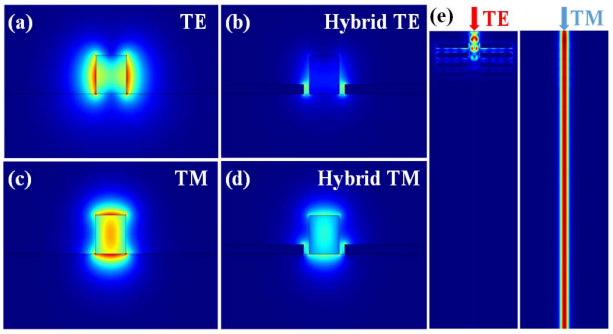

Fig. 4. Normalized electric field distributions of (a, c) dielectric TE and TM mode; (b, d) hybrid plasmonic TE and TM mode. (e) Power distribution along the propagation direction from top view when TE and TM mode is injected respectively. Here, $W = 280$ nm, $g = 50$ nm, and $h_m = 85$ nm.

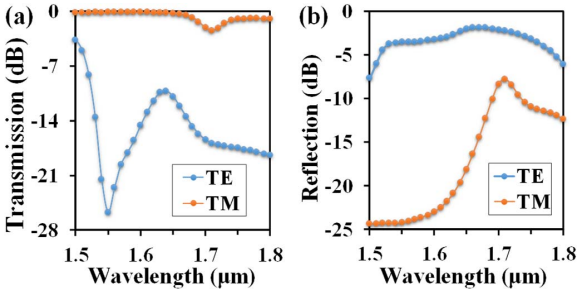

Fig. 5. Wavelength dependence of the transmission (a) and reflection (b) for the proposed TM-pass polarizer.

reflection losses as well. Hence, there is still a possibility that TE polarized light can be reflected and scattered by HPG in several periods. On the other hand, for TM mode, mode overlap increases and Δn_{eff} reduces as h_m decreases, both of which are conducive to reducing the IL. When h_m =85 nm, Δn_{eff} for TM mode is almost zero and mode overlap ratio is as high as 0.98 (Fig. 3), which means reflection loss can be minimized. Therefore, h_m is set to 85 nm as an example.

III. Discussion

The power distributions are illustrated in Figure 4(e) when input TM mode and TE mode separately. 3D FDTD simulation is carried out to further confirm the principle. Here, h_m = 85 nm, W = 280 nm, g = 50 nm, Λ = 500 nm and the operation wavelength is 1.55 μm. The corresponding refractive indices for SiO_2, Si, and Ag are 1.444, 3.478, and 0.145+11.438i [30], respectively. It is obvious that TM mode passes through the HPG while TE mode disappears gradually due to the reflection and SPP stimulation. Two key figures of merit of a polarizer are ER and IL, defined as ER=$10\log_{10}(P_{\mathrm{TM}}/P_{\mathrm{TE}})$, IL= $-10\log_{10}(P_{\mathrm{TM/TE}}/P_{\mathrm{Input}})$, where P_{Input}, P_{TM}, and P_{TE} are the input power, and output power for TM mode and TE mode. In general, small period number results in lower insertion loss because of the less metal absorption for TM mode. In our device, the number of period is chosen to be the smallest value ($N = 5$) while the extinction ratio at 1.55 μm is kept over 20 dB. If we reduce the period number to 4, the ER is less than 19 dB no matter what metal length d is chosen. When period number $N = 5$, grating period $\Lambda = 500$ nm and metal length $d = 260$ nm, the ER reaches the maximum value 25.6 dB with IL only 0.088 dB at 1.55 μm. Although IL can be further reduced by reducing the period number and increasing the gap between metal layer and Si waveguide, the ER will dramatically decrease at the same time.

The wavelength dependence of the transmission and reflection for the proposed TM-pass polarizer is investigated. The transmission for TM polarized light is higher than 0.95 within the wavelength range of (1.45, 1.65) μm. Meanwhile, the transmission for TE mode decreases as wavelength increases and hit bottom at the wavelength of 1.55 μm. The ER is over 10 dB over a large bandwidth of (1.52, 1.8) μm and there is no sign of deterioration beyond 1.8μm (Fig. 5(a)), which is comparable with polarizers reported previously [11], [27]. The elimination of TE mode is achieved by HPG reflection and SPP mode stimulation, and both of the effects are sensitive to the refractive index variation. Since the refractive index of Ag is more sensitive to the wavelength change compared with dielectric material, the transmission of TE mode quickly decreases from its optimum value at other wavelengths. One possible solution is choosing other plasmonic material which is less sensitive to the wavelength change. It is worth noting that the reflection spectrum for TE mode (Fig. 5(b)) is not strictly increasing within the range of (1.53, 1.6) μm and asymmetric, which is different from traditional dielectric based Bragg grating. This is because plasmonic modes are stimulated by the reflected light and part of the energy from reflected light is transferred to SPPs which propagate along the metal surface (Fig. 4(e)). For TM mode, the reflection at 1.55 μm is nearly zero by optimizing parameters and there is one peak at 1.71 μm. Theoretical study shows that the IL is almost wavelength independent and less than 0.1 dB for the whole C-band. It is true that we normally avoid using the present polarizer directly after the light source because the reflection is strong and an isolator or a circulator is needed. However, it is beneficial to improve the ER of the incident TM mode, in which case the reflection of TE mode is negligible. Since the reflection spectrum directly reflects the wavelength range in which the SPPs modes are stimulated, it is useful to design a SPPs generator based on the present polarizer according to the reflection spectrum.

Furthermore, the fabrication tolerance of the proposed device is also analyzed. The waveguide width and metal length variation are important parameters to determine the fabrication tolerance. The device is insensitive to metal length deviation

$$\Gamma = \frac{\left| \frac{1}{4} \iint \left[\vec{E}_{tm} \times \vec{H}^*_{tu} + \vec{E}^*_{tu} \times \vec{H}_{tm} \right]_z dxdy \right|^2}{\frac{1}{4} \iint \left[\vec{E}_{tm} \times \vec{H}^*_{tm} + \vec{E}^*_{tm} \times \vec{H}_{tm} \right]_z dxdy \cdot \frac{1}{4} \iint \left[\vec{E}_{tu} \times \vec{H}^*_{tu} + \vec{E}^*_{tu} \times \vec{H}_{tu} \right]_z dxdy} \tag{4}$$

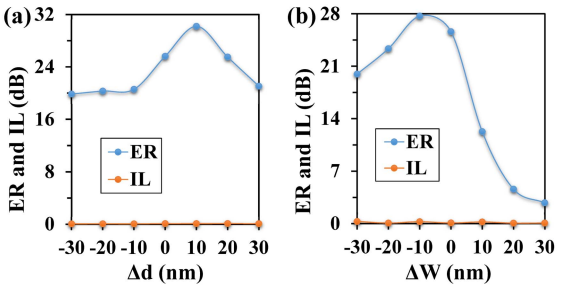

Fig. 6. Dependence of the ER and IL on (a) metal length variation Δd and (b) waveguide width deviation ΔW

Δd since the ER can stay higher than 19 dB and IL is less than 0.1 dB if Δd varies in a range of (-30, 30) nm (Fig. 6(a)). The ER is over 12 dB if waveguide width deviation ΔW varies in a large range of $(-30, 10)$ nm (Fig. 6(b)). We can see that the ER deteriorates rapidly for ΔWover +10 nm, and thus, a slightly narrower waveguide width is preferred. Besides, the IL is lower than 0.3 dB if ΔW varies in a range of $(-30, 30)$ nm.

IV. Conclusion

A low loss, compact TM-pass integrated polarizer is demonstrated using hybrid plasmonic grating structure on SOI platform. At 1.55 μm, the ER is as high as 25.6 dB with compact length of 2.5 μm. Furthermore, the IL is only 0.088 dB which is comparable to dielectric based devices. Because the large mode distribution mismatch and plasmonic effect significantly influence the transmission and reflection spectrum of the device, traditional theory of Bragg grating cannot give a complete explanation. Therefore, we proposed an analysis method which not only effective index but also mode overlap is taken into consideration for the design. Such analysis method can be extended to other structures using Bragg gratings. This device paves the way to realize high-density integration of various applications that need polarization control, such as optical communication, quantum information, and bio-sensing.

References

[1] Q. Deng, Q. Yan, L. Liu, X. Li, J. Michel, and Z. Zhou, "Robust polarization-insensitive strip-slot waveguide mode converter based on symmetric multimode interference," *Opt. Exp.*, vol. 24, no. 7, pp. 7347–7355, Apr. 2016.

[2] L. Liu, Q. Deng, and Z. Zhou, "Subwavelength-grating-assisted broadband polarization-independent directional coupler," *Opt. Lett.*, vol. 41, no. 7, pp. 1648–1651, Apr. 2016.

[3] T. Barwicz *et al.*, "Polarization-transparent microphotonic devices in the strong confinement limit," *Nature Photon.*, vol. 1, no. 1, pp. 57–60, Jan. 2007.

[4] L. Liu, Q. Deng, and Z. Zhou, "Manipulation of beat length and wavelength dependence of a polarization beam splitter using a subwavelength grating," *Opt. Lett.*, vol. 41, no. 21, pp. 5126–5129, Nov. 2016.

[5] L. Gao *et al.*, "On-chip plasmonic waveguide optical waveplate," *Sci. Rep.*, vol. 5, p. 15794, Oct. 2015.

[6] H. Fukuda and K. Wada, "Parallel-core-type polarization rotator for silicon wire waveguide platform," *Photon. Res.*, vol. 2, no. 3, pp. A14–A18, Jun. 2014.

[7] L. Wu, J. Guo, H. Xu, X. Dai, and Y. Xiang, "Ultrasensitive biosensors based on long-range surface plasmon polariton and dielectric waveguide modes," *Photon. Res.*, vol. 4, no. 6, pp. 262–266, Dec. 2016.

[8] C.-H. Chen, L. Pang, C.-H. Tsai, U. Levy, and Y. Fainman, "Compact and integrated TM-pass waveguide polarizer," *Opt. Exp.*, vol. 13, no. 14, pp. 5347–5352, Jul. 2005.

[9] M. Z. Alam, J. S. Aitchison, and M. Mojahedi, "Compact and silicon-on-insulator-compatible hybrid plasmonic TE-pass polarizer," *Opt. Lett.*, vol. 37, no. 1, pp. 55–57, Jan. 2012.

[10] D. Dai, Z. Wang, N. Julian, and J. E. Bowers, "Compact broadband polarizer based on shallowly-etched silicon-on-insulator ridge optical waveguides," *Opt. Exp.*, vol. 18, no. 26, pp. 27404–27415, Dec. 2010.

[11] X. Guan, P. Chen, S. Chen, P. Xu, Y. Shi, and D. Dai, "Low-loss ultracompact transverse-magnetic-pass polarizer with a silicon subwavelength grating waveguide," *Opt. Lett.*, vol. 39, no. 15, pp. 4514–4517, Aug. 2014.

[12] S. Azzam, M. Hameed, N. Areed, M. Abd-Elrazzak, H. El-Mikaty, and S. Obayya, "Proposal of an ultracompact CMOS-compatible TE-/TM-pass polarizer based on SoI platform," *IEEE Photon. Technol. Lett.*, vol. 26, no. 16, pp. 1633–1636, Aug. 15, 2014.

[13] E. Saitoh, Y. Kawaguchi, K. Saitoh, and M. Koshiba, "TE/TM-pass polarizer based on lithium niobate on insulator ridge waveguide," *IEEE Photon. J.*, vol. 5, no. 2, Apr. 2013, Art. no. 6600610.

[14] J. Weifeng and S. Xiaohan, "TE-pass polarizer with cylinder array inserted in buffer layer of silica-on-silicon waveguide," *IEEE Photon. Technol. Lett.*, vol. 26, no. 9, pp. 937–940, May 1, 2014.

[15] Q. Wang and S.-T. Ho, "Ultracompact TM-pass silicon nanophotonic waveguide polarizer and design," *IEEE Photon. J.*, vol. 2, no. 1, pp. 49–56, Feb. 2010.

[16] Y. Xiong, D.-X. Xu, J. H. Schmid, P. Cheben, and W. N. Ye, "High extinction ratio and broadband silicon TE-pass polarizer using subwavelength grating index engineering," *IEEE Photon. J.*, vol. 7, no. 5, Oct. 2015, Art. no. 7802107.

[17] D. K. Gramotnev and S. I. Bozhevolnyi, "Plasmonics beyond the diffraction limit," *Nature Photon.*, vol. 4, no. 2, pp. 83–91, Feb. 2010.

[18] L. Gao, F. Hu, X. Wang, L. Tang, and Z. Zhou, "Ultracompact and silicon-on-insulator-compatible polarization splitter based on asymmetric plasmonic–dielectric coupling," *Appl. Phys. B, Lasers Opt.*, vol. 113, no. 2, pp. 199–203, Nov. 2013.

[19] T.-K. Ng, M. Z. M. Khan, A. Al-Jabr, and B. S. Ooi, "Analysis of CMOS compatible cu-based tm-pass optical polarizer," *IEEE Photon. Technol. Lett.*, vol. 24, no. 9, pp. 724–726, May 1, 2012.

[20] Y. Huang, S. Zhu, H. Zhang, T.-Y. Liow, and G.-Q. Lo, "CMOS compatible horizontal nanoplasmonic slot waveguides TE-pass polarizer on silicon-on-insulator platform," *Opt. Exp.*, vol. 21, no. 10, pp. 12790–12796, May 2013.

[21] M. Alam, J. S. Aitchsion, and M. Mojahedi, "Compact hybrid TM-pass polarizer for silicon-on-insulator platform," *Appl. Opt.*, vol. 50, no. 15, pp. 2294–2298, May 2011.

[22] X. Sun, M. Z. Alam, S. J. Wagner, J. S. Aitchison, and M. Mojahedi, "Experimental demonstration of a hybrid plasmonic transverse electric pass polarizer for a silicon-on-insulator platform," *Opt. Lett.*, vol. 37, no. 23, pp. 4814–4816, Dec. 2012.

[23] T. Huang, "TE-pass polarizer based on epsilon-near-zero material embedded in a slot waveguide," *IEEE Photon. Technol. Lett.*, vol. 28, no. 20, pp. 2145–2148, Oct. 15, 2016.

[24] S. I. Azzam and S. S. A. Obayya, "Titanium nitride-based CMOS-compatible TE-pass and TM-pass plasmonic polarizers," *IEEE Photon. Technol. Lett.*, vol. 28, no. 3, pp. 367–370, Feb. 1, 2016.

[25] X. Guan, P. Xu, Y. Shi, and D. Dai, "Ultra-compact broadband TM-pass polarizer using a silicon hybrid plasmonic waveguide grating," in *Proc. Asia Commun. Photon. Conf.*, 2013, pp. 11–13.

[26] Z. Ying, G. Wang, X. Zhang, Y. Huang, H.-P. Ho, and Y. Zhang, "Ultra-compact TE-pass polarizer based on a hybrid plasmonic waveguide," *IEEE Photon. Technol. Lett.*, vol. 27, no. 2, pp. 201–204, Jan. 15, 2015.

[27] S. Yuan, Y. Wang, Q. Huang, J. Xia, and J. Yu, "Ultracompact TM-pass/TE-reflected integrated polarizer based on a hybrid plasmonic waveguide for silicon photonics," in *Proc. IEEE 11th Int. Conf. Group IV Photon. (GFP)*, Aug. 2014, pp. 183–184.

[28] J. Zhang, E. Cassan, and X. Zhang, "Wideband and compact TE-pass/TM-stop polarizer based on a hybrid plasmonic Bragg grating for silicon photonics," *J. Lightw. Technol.*, vol. 32, no. 7, pp. 1383–1386, Apr. 1, 2014.

[29] J. Buus, M.-C. Amann, and D. J. Blumenthal, *Tunable Laser Diodes and Related Optical Sources*. Hoboken, NJ, USA: Wiley, 2005.

[30] P. B. Johnson and R. W. Christy, "Optical constants of the noble metals," *Phys. Rev. B, Condens. Matter*, vol. 6, no. 12, pp. 4370–4379, Dec. 1972.